1

Potential of the Solar Energy on Mars

Dragos Ronald Rugescu[1] and Radu Dan Rugescu[2]
[1]*University of California at Davis,*
[2]*University Politehnica of Bucharest*
[1]*U.S.A.,*
[2]*Romania E.U.*

1. Introduction

The problem of energy accessibility and production on Mars is one of the three main challenges for the upcoming colonisation of the red planet. The energetic potential on its turn is mainly dependent on the astrophysical characteristics of the planet. A short insight into the Mars environment is thus the compulsory introduction to the problem of energy on Mars. The present knowledge of the Martian environment is the result of more than two centuries of attentive observation on its astronomical appearance and, more recently, on its on-site astrophysical features. Recent surface measurements of Martian geology, meteorology and climate had fixed the sometime-unexpected image of a completely desert planet. Mars is one of the most visible of the seven planets within the solar system and thusfor its discovery cannot be dated, still the interest for Mars is old. It was easily observed from the ancient times by necked eye and the peculiar reddish glance of the planet had induced the common connection of the poor planet with the concept of war. The god of war and the planet that inherited his name had provoked, still from antiquity, curiosity and disputes on the most diverse themes. These disputes are at a maximum right now regarding the habitability of Mars. The red planet owes his color to still unexplained causes, where a yet undisclosed chemistry of iron oxides seems to be the main actor. The visit card of Mars is fast increasing in the quantity of data and is now quite well known (Bizony, 1998), as we observe from the description that follows.

1.1 Mars as seen before the space age

As far as the knowledge of the solar system has gradually extended, from optical, ground-based observations to the present astrophysical research on site, Mars appears as the fourth planet as starting from the Sun. The reddish planet of the skies, nicely visible by necked eyes, has attracted the most numerous comments during the time regarding the presence of life on an extraterrestrial planet. With all other eight planets, except for Pluto-Charon doublet, Mars aligns to a strange rule by orbiting the Sun at a distance that approximates a multiple of $\sqrt{2}$ from that of the Earth. This means that the rough 149.6 mil km of the Earthsemi-major axis is followed by a rough 212 mil km for Mars. In fact there are 227.92 mil

Source: Solar Energy, Book edited by: Radu D. Rugescu,
ISBN 978-953-307-052-0, pp. 432, February 2010, INTECH, Croatia, downloaded from SCIYO.COM

km at mean from the center of Sun. The power rule of Titius-Bode[1], modified several times, but originally described as $a = (4 + 3 \times \mathrm{sgn}\, n \times 2^{n-1}) / 10 \,|\, n = \overline{0,9}$ gives a better distribution,

Planet	n	Titius-Bode rule	Actual semi-major axis
Mercury	0	0.4	0.39
Venus	1	0.7	0.72
Earth	2	1.0	1.00
Mars	3	1.6	1.52
Asteroids	4	2.8	2.80
Jupiter	5	5.2	5.20
Saturn	6	10.0	9.54
Uranus	7	19.6	19.20
Neptune/Pluto	8	38.8	30.10/39.20
Sedna	9	77.2	75.00

Table 1. Mars within Titius-Bode's rule (astronomical units)

It is immediately seen that the primary solar radiation flux is roughly two times smaller for Mars than it is for Earth. More precisely, this ratio is equal to 2.32. This observation for long has suggested that the climate on Mars is much colder than the one on Earth. This has not removed however the belief that the red planet could be inhabited by a superior civilization. Nevertheless, beginning with some over-optimistic allegations of Nicolas Camille Flammarion (*Flamarion*, 1862) and other disciples of the 19-th century, the planet Mars was for a century considered as presenting a sort of life, at least microbial if not superior at all. The rumor of Mars channels is still impressing human imagination. When estimates begun to appear regarding the Martian atmosphere and figures like 50 mbar or 20 mbar for the air pressure on Martian ground were advanced (Jones 2008), a reluctant wave of disapproval has been produced. It was like everybody was hoping that Mars is a habitable planet, that we have brothers on other celestial bodies and the humankind is no more alone in the Universe. As more data were accumulating from spectroscopic observations, any line of emission or absorption on Mars surface was immediately related to possible existence of biological effects. Even during the middle 20-th century the same manner was still preserving. In their book on "Life in the Universe" Oparin and Fesenkov are describing Mars in 1956 as still a potential place for biological manifestations (*Oparin & Fesenkov*, 1956). The following two excerpts from that book are relevant, regarding the claimed channels and biological life on Mars: "...up to present no unanimous opinion about their nature is formed, although nobody questions that they represent real formations on the planet (Mars)..." and at the end of the book "On Mars, the necessary conditions for the appearance and the development of life were always harsher than on Earth. It is out of question that on this planet no type of superior form of vegetal or animal life could exist. However, it is possible for life, in inferior forms, to exist there, although it does not manifest at a cosmic scale."

[1] In 1768, Johann Elert Bode (1747-1826), director of Berlin Astronomical Observatory, published his popular book, "Anleitung zur Kenntnis des gestirnten Himmels" (*Instruction for the Knowledge of the Starry Heavens*), printed in a number of editions. He stressed an empirical law on planetary distances, originally found by J.D. Titius (1729-96), now called "Titius-Bode Law".

The era of great *Mars Expectations*, regarding extraterrestrial life, took in fact its apogee in 1938, when the radio broadcast of Howard Koch, pretending to imaginary fly the coverage of Martian invasion of Earth, had produced a well-known shock around US, with cases of extreme desperation among ordinary people. Still soon thereafter, this sufficed to induce a reversed tendency, towards a gradual diminution of the belief into extraterrestrial intelligence and into a Martian one in particular. This tendency was powered by the fact that no proofs were added in support of any biological evidence for Mars, despite the continuous progress of distant investigations. Still every of the 36 great oppositions of Mars, since the "canali" were considered by Giovanni Schiaparelli in 1877, prior to the space age in 1957, like the series in 1901, 1911, 1941, 1956 was only adding subjective dissemination of channels reports, with no other support for the idea that on Mars any form of biological life exists. After Schiaparelli and Flammarion, the subjective belief in a Martian life is successively claimed by the well known astronomers Antoniadi, Percival Lowel, A. Dollfus, G. A. Tihov and others.

Any documentation of a hostile environment on Mars was received with adversity. Despite later spectroscopic and radiometric measurements from Earth, which were revealing a very thin atmosphere and extreme low temperatures, still in the immediate down of the space age the pressure on the Martian soil was yet evaluated at 87 mbar (*Oparin & Fesenkov*, 1956), overrating by more than ten times the actual value, irrefutably found after 1964. It is a pregnant evidence of how subjective the world could be in administrating even the most credible scientific data in this delicate subject. A piece of this perception is surviving even today.

1.2 Mars during the space age

With the availability of a huge space carrier, in fact a German concept of Görtrupp, the Soviets started to built a Mars spacecraft during 1959, along to the manned spacecraft Vostok. The launch took place as early as in October 1960, mere 3 years after Sputnik-1, but proved that only mechanical support is of no much use. The restart of the accelerator stage from orbit was a failure that repeated a few weeks later with similar non-results. The boost towards Mars commenced again with Mars-1 and a companion during the 1962 window, ending in failure again. It followed this way that a much smaller but smarter US device, called Mariner-4, despite of the nose-hood miss-separation of its companion Mariner-3, had marked the history of Mars in 1964 with a shaking fly-by of the planet and several crucial observations. These stroke like a thunder: the radio occultation experiment was suddenly revealing an unexpectedly low atmospheric pressure on Mars of approximately 5 mbar, much far below the most of the previous expectations. The life on Mars was bluntly threatened to became a childish story. Primitive but breathtaking images from Mariner-4 were also showing a surface more similar to the Moon's one than any previous expectation could predict. A large number of craters were mixed with dunes and shallow crevasses to form a desert landscape and this appearance produced a change in the perception of the formation of the solar system at large. No channel was revealed and none of the previously mentioned geometrical marks on the Martian surface. The wave of disappointment grew rapidly into a much productive bolster for deepening these investigations, so incredible those results were. Mars's exploration proceeded with Mariner-6 and 7 that performed additional Martian fly-byes in 1967 only to confirm the portrait of a fully deserted planet.

The present hostile environment on Mars and the absence of life seem for now entirely proven, but it still remains to understand when this transform took place, whether there was sometime a more favorable environment on Mars and all issues regarding the past of Mars.
We say *for now* because our human nature bolsters us towards an ideal which we only dream of, but which, as we shall prove, is almost accomplishable to the level of present technologies. Anyhow, the nephews of our nephews will perhaps take it up to the end. We are speaking of Mars's colonization, process that could only take place after the complete transformation of the surface and of the atmosphere to closely resemble those on Earth, process we call terraforming. Whether planet Mars worth more than its terraforming, then it deserves all the money spent with this process.
For the moment however, the Martian environment is far of being earth-like, as the compared data from the next table reveal (*Almanac* 2010):

Parameter	Mars	Earth	units.
Orbital eccentricity	ε = 0,09341233	0.01669518	-
Semi-major axis	a = 227,920,000	149,597,871	km
Focal semi-chord	p = 225,931,201	149,556,174	km
Perihelion	r_P= 206,629,462	147,100,308	km
Aphelion	r_A= 249,210,538	152,095,434	km
Inclination to ecliptic	i = 1.84964^o	0^o	^{o}
Ascending node	Ω = 49.6296364^o	0^o	^{o}
Perihelion argument	ω = 336.04084^o	102.94719^o	^{o}
Sideral revolution	T = 59355072	31558118	s
Equatorial radius	R_e= 3,397,515.0*	6,378,136.6	m
Flattening factor	f = 1/154.321	1/298.25642	-
Rotational velocity	w =7.088244 ·10^{-05}	7. 292700 ·10^{-05}	rad/s
Obliquity	v = 25.19^o	23.45^o	^{o}
Gravitational field**	K = 4.28283149 ·10^4	3.986004391 ·10^5	km^3/s^2
Solar irradiance	q = 589.2	1367.6	W/m^2
Ground pressure***	p_0 = 6.36	1013.25	mbar
Ground temperature	T_0= 210.0	283.0	^{o}K .

* (JPL 1998)
** Earth without Moon
*** Mean for Martian latitude and year

Table 2. Comparative Mars and Earth astrophysical data

The data in table 2 are based on the mean eccentricities of the year 2009 as given in the reference. Accordingly, a value of g=6.67428 ·10^{-11} is used for the universal constant of gravitation. Second is the time unit used to define the sidereal periods of revolution around the Sun and is derived, on its turn, from the solar conventional day of 24 hours in January 1, 1900. The atmosphere of Mars is presently very well known and consists, in order, of Carbon dioxide (CO_2) 95.32%, Nitrogen (N_2) 2.7%, Argon (Ar) 1.6%, Oxygen (O_2) 0.13%, Carbon monoxide (CO) 0.07%, Water vapor (H_2O) 0.03%, Nitric oxide (NO) 0.013%, Neon (Ne) 2.5 ppm, Krypton (Kr) 300 ppb, Formaldehyde (H_2CO) 130 ppb [1], Xenon (Xe) 80 ppb, Ozone (O_3) 30 ppb, Methane (CH_4) 10.5 ppb and other negligible components. This composition is further used to assess the effect of solar radiation upon the dissociation and los of the upper Mars atmosphere and upon potential greenhouse gases.

The present atmosphere of Mars is extremely tenuous, below 1% of the Earth one and seemingly unstable. Seasonal worming and cooling around the poles produce variations of up to 50% in atmospheric pressure due to carbon dioxide condensation in winter. The values in table 18.2 are rough means along an entire year, as measured by Viking-1 and Viking-2 lenders, Pathfinder and Phoenix station recently. The greenhouse effect of carbon dioxide is considered responsible for 5° increment of atmospheric temperature, very low however, with only occasional and local worming above 0°C on privileged equatorial slopes. The chart of the present Martian atmosphere (*Allison & McEwen*, 2000) is given in figure 18.1. The exponential constant for pressure on Mars is H=11,000 m.

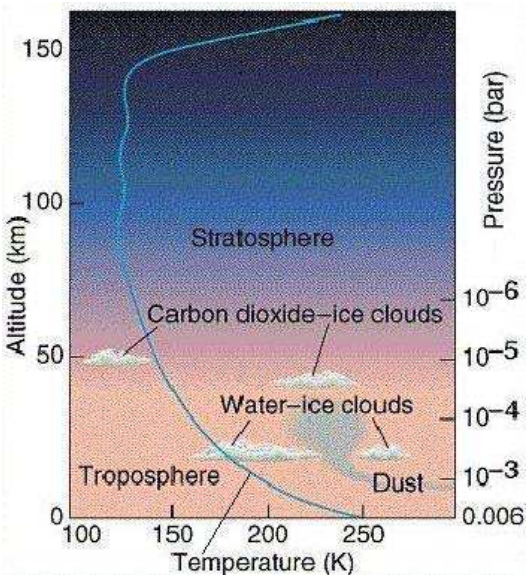

Fig. 1. Mars's atmosphere profile.

These atmospheric characteristics stand as the database in evaluating the efficiency of the solar-gravitational draught, closed-circuit powerplant, which we propose to be employed as an energy source on Mars.

1.3 Mars presumptive past

It is generally considered that the planetary atmospheres, including that of Mars, went through major transformations at the beginning of formation of the solar system (Brain 2008). Present models show a gradual and fast depletion of Martian atmosphere, with essential implications for designing the Mars's terraforming. Even today, the depletion of Mars's atmosphere continues on a visible scale. The observations, recently made by Mars Express and Venus Express, have allowed scientists to draw similar conclusions for both Mars and Venus, through direct comparisons between the two planets. The phenomenon proves this way as nonsingular and systematic (*Brain,* 2008). The results have shown that both planets release beams of electrically charged particles to flow out of their atmospheres. The particles are being accelerated away by interactions with the solar wind released by the Sun. This phenomenon was observed by the two spacecrafts while probing directly into the

magnetic regions behind the planets, which are the predominant channels through which electrically-charged particles escape. The findings show that the rate of escape rose by ten times on Mars when a solar storm struck in December 2006. Despite the differences among the two atmospheres, the magnetometer instruments have discovered that the structure of the magnetic fields of both planets is alike. This is due to the fact that the density of the ionosphere at 250 km altitude is surprisingly similar, as shows the Venus Express magnetometer instrument. By observing the current rates of loss of the two atmospheres, planetary scientists try to turn back the clock and understand what they were like in the past. To build a model of Mars's atmosphere past we are only basing our presumptions on the in-situ observed tracks impressed by that past evolution. A very detailed computer modeling of the charged particles erosion and escape may be found in a recent paper from Astrobiology (*Terada et al.*, 2009), with the tools of magneto-fluid-dynamics and today's knowledge of the Martian upper atmosphere and of the solar radiation intensity.

First, recent orbital observations of networks of valleys in high lands and cratered areas of the Southern Hemisphere, especially those by Mars Express and Mars suggest that Mars exhibited a significant hydrologic activity during the first Gyr (Giga-year) of the planet lifetime. Some suggest that an ancient water ocean equivalent to a global layer with the depth of about 150 m is needed for the explanation of the observed surface features (*Bullock & Moore*, 2007). These authors suppose that the evolution of the Martian atmosphere and its water inventory since the end of the magnetic dynamo (*Schubert et al.*, 2000) at the late Noachian period about 3.5-3.7 Gyr ago was dominated by non-thermal atmospheric loss processes. This includes solar wind erosion and sputtering of oxygen ions and thermal escape of hydrogen (*Zhang et al.*, 1993). Recent studies (*Wood at al.*, 2005) show that these processes could completely remove a global Martian ocean with a thickness of about 10–20 m, indicating that the planet should have lost the majority of its water during the first 500 Myr. As far as Mars was exposed before the Noachian period to asteroid impacts, as the entire solar planets did, their effect on atmospheric erosion was simulated. Furthermore, the study uses multi-wavelength observations by the ASCA, ROSAT, EUVE, FUSE and IUE satellites of Sun-like stars at various ages for the investigation of how high X-ray and EUV fluxes of the young Sun have influenced the evolution of the early Martian atmosphere. Terada et al. apply for the first time a diffusive-photochemical model and investigate the heating of the Martian thermosphere by photo-dissociation and ionization processes and by exothermic chemical reactions, as well as by cooling due to CO_2 IR-radiation loss. The model used yields high exospheric temperatures during the first 100–500 Myr, which result in blow off for hydrogen and even high loss rates for atomic oxygen and carbon. By applying a hydrodynamical model for the estimation of the atmospheric loss rates, results were obtained, which indicate that the early Martian atmosphere was strongly evaporated by the young Sun and lost most of its water during the first 100 – 500 Myrs after the planets origin. The efficiency of the impact erosion and hydrodynamic blow off are compared, with the conclusion that both processes present the same rating.

It is a common believe now that during the early, very active Sun's lifetime, the solar wind velocity was faster then the one recorded today and the solar wind mass flux was higher during this early active solar period (Wood *et al.*, 2002, 2005; Lundin *et al.*, 2007).

As the solar past is not directly accessible, comparisons to neighboring stars of the same G and K main-sequence, as observed e. g. By the Hubble Space Telescope's high-resolution spectroscopic camera of the H Lyman-α feature, revealed neutral hydrogen absorption associated with the interaction between the stars' fully ionized coronal winds and the

partially ionized interstellar medium (Wood *et al*. 2002, 2005). These observations concluded in finding that stars with ages younger than that of the Sun present mass loss rates that increase with the activity of the star. A power law relationship was drawn for the correlation between mass loss and X-ray surface flux, which suggests an average solar wind density that was up to 1000 times higher than it is today (see Fig. 2 in Lammer *et al*., 2003a).

This statement is considered as valid especially for the first 100 million years after the Sun reached the ZAMS (Kulikov *et al*. 2006, 2007), but not all observations agree with this model. For example, observations by Wood *et al.* (2005) of the absorption characteristic of the solar-type G star τ-Boo, estimated as being 500-million-year-old, indicate that its mass loss is about 20 times less than the loss rate given by the mass loss power law, for a star with a similar age. Young stars of similar G- and K-type, with surface fluxes of more than 10^6 erg/cm^2/s require more observations to ascertain exactly what is happening to stellar winds during high coronal activity periods. Terada *et al*. (2009) are using a lower value for the mass loss, which is about 300 times larger than the average proton density at the present-day Martian orbit. These high uncertainties regarding the solar wind density during the Sun's youth prevent from attracting a confident determination of how fast the process of atmospheric depletion took place. To overcome this uncertainty, Terada *et al*. (2009) has applied a 3-D multispecies MHD model based on the Total Variation Diminishing scheme of Tanaka (1998), which can self-consistently calculate a planetary obstacle in front of the oncoming solar wind and the related ion loss rates from the upper atmosphere of a planet like Mars.

Recently, Kulikov *et al*. (2006, 2007) applied a similar numerical model to the early atmospheres of Venus and Mars. Their loss estimates of ion pickup through numerical modeling strongly depended on the chosen altitude of the planetary obstacle, as for a closer planet to the star more neutral gas from the outer atmosphere of the planet can be picked up by the solar plasma flow. We shall give here a more developed model of the rarefied atmosphere sweeping by including the combined effect of electrically charged particles and the heterogeneous mixture of gas and fine dust powder as encountered in the Martian atmosphere along the entire altitude scale.

Data were sought from the geology of some relevant features of the Mars surface like the Olympus Mons (Phillips *et al.*, 2001; Bibring *et al*., 2006), the most prominent mountain in the solar system, to derive an understanding of the past hydrology on the red planet and the timing of geo-hydrological transformations of the surface. Olympus Mons is an unusual structure based on stratification of powdered soils. To explain the features, computer models with different frictional properties were built (McGovern and Morgan, 2009). In general, models with low friction coefficient reproduce two properties of Olympus Mons' flanks: slopes well below the angle of repose and exposure of old, stratigraphically low materials at the basal scarp (Morris and Tanaka, 1994) and distal flanks (Bleacher et al., 2007) of the edifice. The authors show that such a model with a 0.6° basal slope produces asymmetries in averaged flank slope and width (shallower and wider downslope), as actually seen at Olympus Mons. However, the distal margins are notably steep, generally creating planar to convex-upward topography.

This is in contrast to the concave shape of the northwest and southeast flanks and the low-slope distal benches (next figure) of Olympus Mons. Incremental deformation is concentrated in the deposition zone in the center of the edifice.

Outside of this zone, deformation occurs as relatively uniform outward spreading, with little internal deformation, as indicated by the lack of discrete slip surfaces. This finding

contradicts the evidence for extension and localized faulting in the northwest flank of Olympus Mons. The wedgelike deformation and convex morphology seen in the figure appear to be characteristic of models with constant basal friction. McGovern and Morgan (2009) found that basal slopes alone are insufficient to produce the observed concave-upward slopes and asymmetries in flank extent and deformation style that are observed at Olympus Mons; instead, lateral variations in basal friction are required.

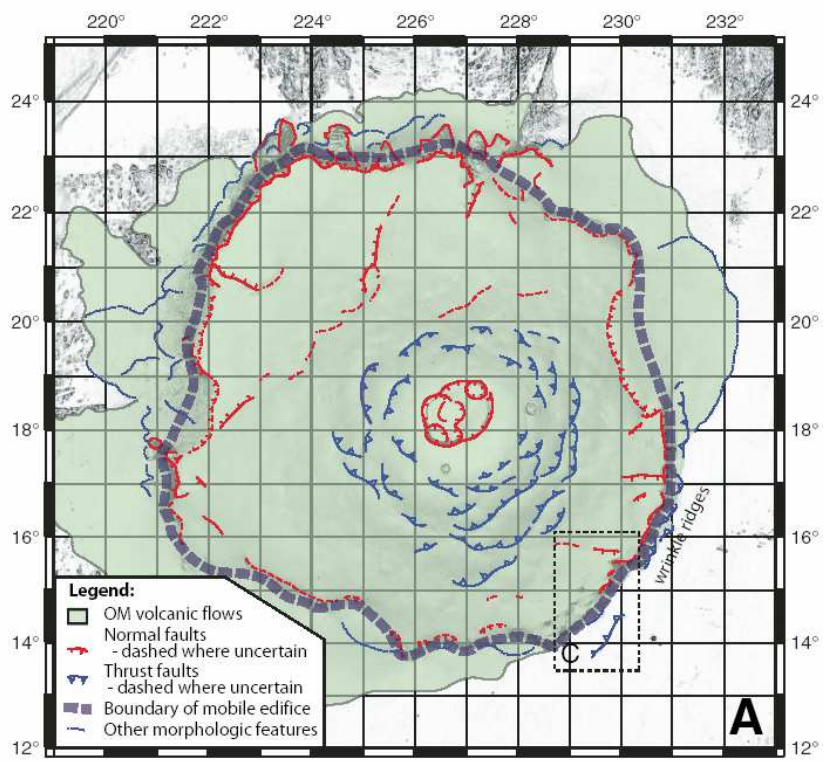

Fig. 2. Geology and interpretation of the Olympus Mons.

The conclusion is that these variations are most likely related to the presence of sediments, transported and preferentially accumulated downslope from the Tharsis rise. Such sediments likely correspond to ancient phyllosilicates (clays) recently discovered by the Mars Express mission. This could only suggest that liquid water was involved into the formation of ancient Olympus Mons, but neither of the conclusions of this work is strong enough. Up to the present, those findings are some of the hardest arguments for ancient water on Mars for a geologically long period.

The importance of this finding is in the promise that a thick atmosphere and wet environment could have been preserving for a long period and thus the Earth-like climate could withstand the depletion influences long enough. This is the type of encouraging arguments that the community of terraforming enthusiasts are waiting for. Problems are still huge, starting with the enormous amounts of energy required for the journey to Mars and back.

2. Energy requirements for the Earth-Mars- Earth journey

The problem of transportation from Earth to Mars and vice versa are restricted by the high amount of energy that must be spent for one kg of payload to climb into the gravitational field of the Sun up to the Mars level orbit and back to the Earth's orbit, where the difference in the orbital speed must also be zeroed. Astrophysical data from the first paragraph allow computing exactly this amount of energy. With the inertial, reactive propulsion of today, two strategies of transferring from Earth to Mars are possible and they belong to the *high thrust navigation* and to *low thrust navigation*. The energy requirements we consider are those for transfer from a low altitude, circular orbit around the starting planet to the low altitude, circular orbit around the destination planet. The very energy of injection into the corresponding low orbits should be added as a compulsory and given extra quantity, as far as the fragmentation of flight for pausing into a transfer orbit neither adds nor diminishes the energetic consumption of the total flight. It remains to determine the energy consumption for the transfer itself.

The motion into a field of central forces always remains planar and is easily describer in a polar, rotating referential by the equation of Binet (Synge and Griffith, 1949), based on the polar angle θ, named the *true anomaly*. For a gravitational field this equation reads

$$\frac{d^2u}{d\theta^2} + u = \frac{K}{h^2u^2} \tag{1}$$

The solution is a conical curve $r(\theta)$ that may be an ellipse, parabola or hyperbola, depending on the initial position and speed of the particle. The expression of the orbit equation may be found while resuming the Cartesian, planar orthogonal coordinates $\{x\mathrm{O}y\}$, where the position vector and the velocity are given by (Mortari, 2001)

$$\mathbf{r} = \frac{p}{1+\varepsilon\cos\theta}\begin{bmatrix}\cos\theta\\ \sin\theta\end{bmatrix},\ \mathbf{v} = \sqrt{\frac{K_\oplus}{p}}\begin{bmatrix}-\sin\theta\\ e+\cos\theta\end{bmatrix}. \tag{2}$$

Between the local position on the conical orbit and the corresponding orbital velocity the relation exists, that derives from the conservation of energy or simply by calculating the velocity from the integral of the equation of motion, in this case with the Earth gravitational parameter $K_\oplus$,

$$\mathbf{v} = \sqrt{\frac{K_\oplus}{p}}\cdot\frac{1+e\cos\varphi}{p}\begin{bmatrix}0 & -1\\ 1 & \dfrac{e}{\sin\varphi}\end{bmatrix}\cdot\mathbf{r}\,. \tag{3}$$

Multiplying the matrices and considering the case when the orbital eccentricity lies between 0 and 1, that means elliptical orbits, the usual energy equation of the orbital speed appears (Synge and Griffith, 1949)

$$v^2 = K_\oplus\left(\frac{2}{r} - \frac{1}{a}\right). \tag{4}$$

These formulae are only needed to access the energy requirements for an impulsive transfer towards Mars and thus a so-called high thrust interplanetary transfer is resulting. The

results supplied this way are bound to some approximations when considering the Earth-Mars actual transfer. They mainly come from the fact that the two planets move along slightly non-coplanar orbits, the angle between the two orbital planes is that given in Table 18.2, namely the inclination of Mars's orbit to the ecliptic is

$$i = 1.84964^{o}.$$

This circumstance induces a very little difference in the transfer energy however and all previous results from the coplanar approximation preserve quite correct.

2.1 Energy for Earth-Mars high thrust transfers

With moderately high thrust propulsion the acceleration for the transfer acts quick and the time of flight gets its actual minimum. The amount of energy is directly given by the equation of motion on the quasi-best, quasi-Hohmann transfer orbit that starts from around the Earth and ends around Mars (figure below).

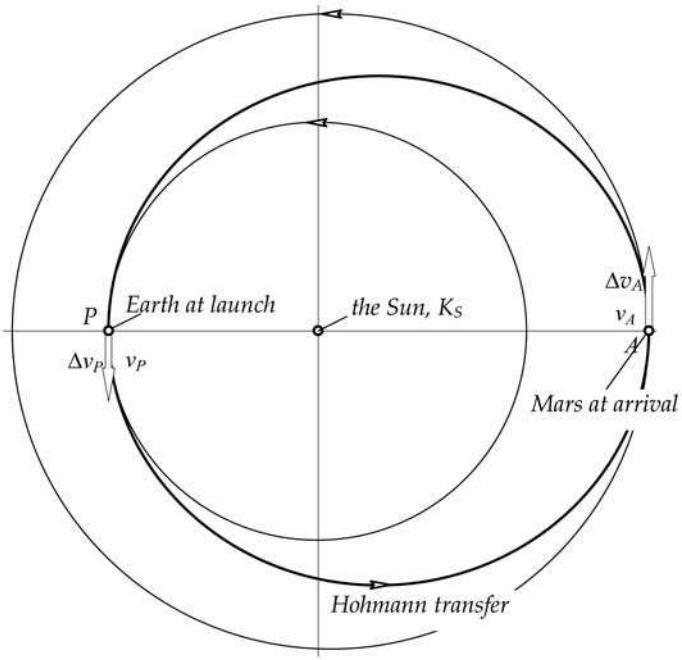

Fig. 3. Minimum energy Earth-Mars transfer

To enter the higher altitude orbit as referred to the Sun, the transfer spacecraft must be provided with extra kinetic energy at the Earth orbit level, exactly equal to the perihelion energy of the transfer Hohmann ellipse, v_P^2. This difference is easily computed by using equation (4).

When we introduce the gravitational parameter of the Sun $K_\odot$ and the location of the perihelion at Earth orbit level r_P, the extra speed required to the spacecraft is $\Delta v_P = v_P - v_E = 32.746 - 29,7944 = 2.952$ km/s. With the same procedure we observe that at the arrival on Mars orbit level, the spacecraft requires additional energy and speed to remain on the Mars

orbit level around the Sun, namely $\Delta v_A = v_M - v_A$=24,126-21,472=2.654 km/s. The total velocity requirement for the spacecraft equals the considerable amount of Δv_Σ=5.606 km/s.
To this requirement the exit energy from the Earth gravity and the braking energy to avoid fall on Mars must be added. In order to remain with the required extra velocity when the spacecraft leaves the Earth field of gravity, the semi-axis of the departure hyperbola must comply with the value given by

$$v_\infty^2 = K_\oplus \left(\frac{1}{a_{\oplus e}} \right) = 2.952^2 \tag{5}$$

from where the value results,

$$a_{\oplus e} = K_\oplus / 8.714304 = 45759.478 \text{ km} \tag{6}$$

with the corresponding hyperbolic escape velocity at the altitude of a LEO (*Low Earth Orbit*, h=200 km) of

$$v_e^2 = K_\oplus \left(\frac{2}{R_0 + h} + \frac{1}{a_{\oplus e}} \right) = 130.14 \tag{7}$$

from where the value results

$$v_e = 11.408 \text{ km/s}$$

that must be actually supplied to the spacecraft to properly initiate the transfer to Mars. The local parabolic velocity were v_2=11.019 km/s only.
At the Mars end of the flight, the spacecraft is challenged with a continuous fall towards Mars, as it enters the gravitational field of Mars with a hyperbolic velocity at infinity of 2.654 km/s. Similar computations show that at Mars arrival, namely at an altitude of merely 50 km above the Martian surface, where the aerodynamic breaking begins to manifest, the velocity relative to Mars raises to 5.649 km/s and must be completely slowed down. These transfer velocities are ending in 17.057 km/s.
The high amount of energy at approach and landing on Mars can be diminished by air breaking, at least in part. It only remains then to assure the launching velocity from Earth, with its considerable amount. In terms of energy, this requirement equals 65 MJ for each kilogram of end-mass in hyperbolic orbit, to which the energy for lifting that kilogram from the ground to the altitude of the orbit must be considered. This extra energy of less than 2 MJ looks negligible however, as compared to the kinetic energy requirement from above.
It must be considered that a value of 16 MJ only is required for the return travel to Earth from MLO (Mars low orbit). It is thus hard to understand the reasoning for the so-called *one-way trips to Mars*, or to be open "*no return trips to Mars*", warmly proposed by some experts in Mars colonization from Earth.

3. A thick atmosphere facing erosion

Long term events in the outer atmosphere of the planet are related to the interaction of the solar radiation and particles flow (solar wind) with the very rarefied, heterogeneous fluid envelope of the planet. A model of an electrically charged gas was recently used by Tanaka et al. (2009) to approach the erosion rate of the Martian atmosphere under high UV solar

radiation. We add now the double phase fluid model that covers the dust dispersion proved even in 1975 by the Viking spacecraft to flow at high altitudes into the tinny atmosphere. First the equations of conservation and motion for the heterogeneous and rarefied fluid should be introduced.

3.1 Equations governing the exo-atmospheric erosion

While writing the equations of motion of a material particle of the rarefied gas and its condensed, particle content the relative referential related to the moving planet is considered. The equations of motion, referenced to a non-inertial coordinate system, depend on the relative acceleration of the particles and thus on the *transport* and *complementary* acceleration terms, given by Rivals and Coriolis formulae (Rugescu, 2003)

$$\begin{aligned} \mathbf{a}_t &= \mathbf{a}_{\mathrm{M}} + \left(\boldsymbol{\Omega}_t^2 + \boldsymbol{\Omega}_t'\right)\cdot\mathbf{x}, \\ \mathbf{a}_{\mathrm{C}} &= 2\,\boldsymbol{\Omega}_t \wedge \mathbf{v}, \end{aligned} \tag{8}$$

where $\boldsymbol{\Omega}_t$ is the anti-symmetric matrix of the transport velocity (rotation). Four distinct types of time derivatives exist when the relative fluid motion is described (Rugescu, R. D., 2000). With an apostrophe for the absolute, total (material) time derivative and d/dt for the local total time derivative the vectors and associated matrices of relative motion are

$$\begin{aligned} &\mathbf{r} = \begin{pmatrix} x \\ y \\ z \end{pmatrix}, \quad \mathbf{v} \equiv \begin{pmatrix} u \\ v \\ w \end{pmatrix} = \frac{d\mathbf{r}}{dt}, \quad \mathbf{a} \equiv \begin{pmatrix} a \\ b \\ c \end{pmatrix} = \frac{d^2\mathbf{r}}{dt^2}, \\ &\boldsymbol{\omega}_t = \begin{pmatrix} \omega_x \\ \omega_y \\ \omega_z \end{pmatrix}, \quad \boldsymbol{\Omega}_t = \begin{bmatrix} 0 & -\omega_z & \omega_y \\ \omega_z & 0 & -\omega_x \\ -\omega_y & \omega_x & 0 \end{bmatrix}. \end{aligned} \tag{9}$$

Only the centripetal component $\mathbf{a}_c = -\boldsymbol{\Omega}_t^2 \cdot \mathbf{r}$ preserves the direction of the position vector **r**, the other components presenting ortho-normal properties.

Consequently, the global effect of the relative, non-inertial motion upon the acoustical behavior of the fluid can only be described in a computational 3-Dimensional scheme, although partial effects can be evaluated under simpler assumptions.

The twin viscosity coefficient model observes the reology of the fluid with coefficients of viscosity introduced. The following NS-type, laminar, unsteady hyperbolic matrix equation system is written for both the gas fraction and the condensed part of the fluid mixture, and stands for example as the background of the *Eagle* solver (Tulita et al., 2002), used in many previous aerodynamic investigations at QUB and UPB. A single type of condensed particles is considered, in other words the chemical interactions are seen as minimal and not interfering with the flow process.

To express more precisely the conservation of the gas and particles that fill the same elemental volume dV we observe that a fraction only α of the lateral area of the frontier is occupied by the gas, while the remaider fraction (1-α) is traversed by the condensed particles. Consequently, the area where the pressure acts upon the gas is αA_i for each facet of the cubic volume element (Fig. 4).

In orthogonal and 3D non-inertial coordinates this equations write out for the gas fraction and for the condensate as:

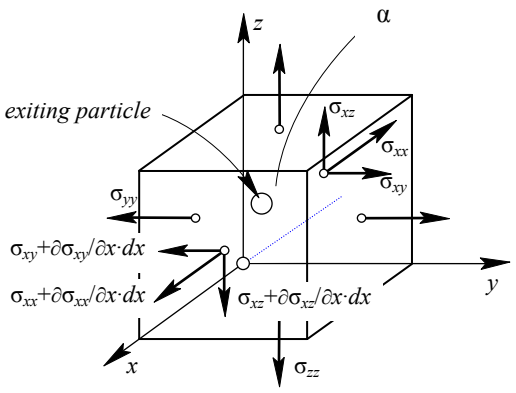

Fig. 4. The heterogeneous fluid

$$\frac{\partial \mathbf{E}}{\partial t}+\frac{\partial \mathbf{F}}{\partial x}+\frac{\partial \mathbf{G}}{\partial y}+\frac{\partial \mathbf{H}}{\partial z}+\mathbf{K}=\mathbf{0}\,, \tag{10}$$

$$\iiint_{ATR}\left[\left(\frac{\partial E}{\partial t}+\frac{\partial F}{\partial x}+\frac{\partial G}{\partial y}+\frac{\partial H}{\partial z}\right)M_p f+K\right]dR\,dT\,dA=0\,, \tag{11}$$

where the vectors are used as defined by the following expressions, in connection with the above system (3) and (4):

$$\mathbf{E}=\begin{bmatrix}\rho\\ \rho u\\ \rho v\\ \rho w\\ \rho h-p\\ \rho_c\end{bmatrix}, \tag{12}$$

$$\mathbf{F}=\begin{bmatrix}\rho u\\ \rho u^2+\alpha p-2\mu\alpha\dfrac{\partial u}{\partial x}-\alpha\left(\dfrac{\mu}{3}+\mu'\right)\nabla\cdot\mathbf{V}\\ -\alpha\mu\left(\dfrac{\partial v}{\partial z}+\dfrac{\partial w}{\partial y}\right)\\ -\alpha\mu\left(\dfrac{\partial w}{\partial x}+\dfrac{\partial u}{\partial z}\right)\\ \rho hu-\lambda\dfrac{\partial T}{\partial x}\\ \iiint\limits_{\mathbf{v}_p TR} M_p(R)f\,dR\,dT\,d\mathbf{v}_p\end{bmatrix}, \tag{13}$$

$$\mathbf{G}=\begin{bmatrix} \rho v \\ -\mu\alpha\left(\dfrac{\partial u}{\partial y}+\dfrac{\partial v}{\partial x}\right) \\ \rho v^2+\alpha p-2\alpha\mu\dfrac{\partial v}{\partial y}-\alpha\left(\dfrac{\mu}{3}+\mu'\right)\nabla\cdot\mathbf{V} \\ -\alpha\mu\left(\dfrac{\partial w}{\partial y}+\dfrac{\partial v}{\partial z}\right) \\ \rho hv-\lambda\dfrac{\partial T}{\partial y} \\ \iiint\limits_{\mathbf{v}_p TR} M_p(R) f\, dR\, dT\, d\mathbf{v}_p \end{bmatrix}, \tag{14}$$

$$\mathbf{H}=\begin{bmatrix} \rho w \\ -\mu\alpha\left(\dfrac{\partial u}{\partial z}+\dfrac{\partial w}{\partial x}\right) \\ -\alpha\mu\left(\dfrac{\partial v}{\partial z}+\dfrac{\partial w}{\partial y}\right) \\ \rho w^2+\alpha p-2\alpha\mu\dfrac{\partial w}{\partial z}-\alpha\left(\dfrac{\mu}{3}+\mu'\right)\nabla\cdot\mathbf{V} \\ \rho hw-\lambda\dfrac{\partial T}{\partial z} \\ \iiint\limits_{\mathbf{v}_p TR} M_p(R) f\, dR dT\, d\mathbf{v}_p \end{bmatrix}, \tag{15}$$

$$\mathbf{K}=\begin{bmatrix} 0 \\ \gamma_{Mx}+z\omega'_y-y\omega'_z+\omega_x(y\omega_y+z\omega_z)-x(\omega_y^2+\omega_z^2)+ \\ +2(w\omega_y-v\omega_z)-\rho f_x+S_x \\ \gamma_{My}+x\omega'_z-z\omega'_x+\omega_y(z\omega_z+x\omega_x)-y(\omega_z^2+\omega_x^2)+ \\ +2(u\omega_z-w\omega_x)-\rho f_y+S_y \\ \gamma_{Mz}+y\omega'_x-x\omega'_y+\omega_z(x\omega_x+y\omega_y)-z(\omega_x^2+\omega_y^2)+ \\ +2(v\omega_x-u\omega_y)-\rho f_z+S_z \\ -\mathbf{V}\cdot\nabla p-\mathbf{\Pi}:\nabla\circ\mathbf{V}+S \end{bmatrix} \tag{16}$$

The following notations were used in the expression of the vector **K**, referring to the distribution of condensed particles:

$$S_x\equiv\iiint\limits_{u_p TR}\left(\frac{9}{2}\frac{\mu_g c}{\rho_p R^2}-3\frac{d\ln R}{dt}-\frac{d\ln f}{dt}\right)(u-u_p)M_p f(x,r,T,u_p,t)dRdT\,du_p\,,$$

$$S_y \equiv \iiint_{v_p\,TR}\left(\frac{9}{2}\frac{\mu_g c}{\rho_p R^2}-3\frac{d\ln R}{dt}-\frac{d\ln f}{dt}\right)(v-v_p)M_p f(x,r,T,u_p,t)dR\,dT\,dv_p\,,$$

$$S_z \equiv \iiint_{w_p\,TR}\left(\frac{9}{2}\frac{\mu_g c}{\rho_p R^2}-3\frac{d\ln R}{dt}-\frac{d\ln f}{dt}\right)(w-w_p)M_p f(x,r,T,u_p,t)dR dT\,dw_p\,,$$

$$S \equiv \iiint_{\mathbf{v}_p\,TR}\left\{\left(e_p+v_p^2/2\right)D_p-\left[A_p(\mathbf{v}-\mathbf{v}_p)^2+B_p\right]M_p f(x,r,T,u_p,t)\right\}dR dT\,d\mathbf{v}_p\,.$$

The equations involving the solid phase (dust particles) depend upon the distribution of the particles along their size, temperature, velocity and their distribution in space as a variable of time. Consequently some extra terms in the four expressions from above are to be written for those functions as follows:

$$A=\begin{bmatrix}u_p\\v_p\\w_p\\\mathbf{v}_p\end{bmatrix},\ E=\begin{bmatrix}u_p\\v_p\\w_p\\M_p f(h_p+\mathbf{v}_p^2)\end{bmatrix},\ F=\begin{bmatrix}u_p^2\\u_p v_p\\u_p w_p\\M_p f(h_p+\mathbf{v}_p^2)u_p\end{bmatrix} \tag{17}$$

$$G=\begin{bmatrix}u_p v_p\\v_p^2\\v_p w_p\\M_p f(h_p+\mathbf{v}_p^2)v_p\end{bmatrix},\ H=\begin{bmatrix}u_p w_p\\v_p w_p\\w_p^2\\M_p f(h_p+\mathbf{v}_p^2)w_p\end{bmatrix}, \tag{18}$$

$$K=\begin{bmatrix}A_p(u-u_p)-f_x\\A_p(v-v_p)-f_y\\A_p(w-w_p)-f_z\\\left[(h_p+\mathbf{v}_p^2)\nabla\cdot\mathbf{v}_p+B_p-2\mathbf{v}_p\cdot\mathbf{f}\right]M_p f\end{bmatrix}. \tag{19}$$

Other three simplifying notations were used to define the factors from the vector (18.19) as follows:

$$A_p \equiv \frac{9}{2}\frac{\mu_g c}{\rho_p R^2}-3\frac{d\ln R}{dt}-\frac{d\ln f}{dt} \tag{20}$$

$$B_p \equiv \frac{3}{\rho_p R_p}\left[\alpha_c(T_p-T)+\sigma_0\left(\varepsilon_p T_p^4-\varepsilon T^4\right)\right] \tag{21}$$

$$D_p \equiv \frac{d\left(M_p f_p\right)}{dt}+M_p f_p\nabla\cdot\mathbf{v}_p \tag{22}$$

While ionization is acting on the rarefied fluid the terms including the external, field forces include the Lorenz forces that appear in the fluid. Coefficients and properties of the field parameters are taken into account within the model developed by Terada (Terada et al. 2009),

Solar wind parameters	*Present*	*4.5 Ga*
Solar wind proton density	3 cm^{-3}	1000 cm^{-3}
Solar wind velocity	450 km s^{-1}	2000 km s^{-1}
B_{IMF} (Parker spiral)	2 nT	60 nT
XUV flux (normalized to martian orbit)	1 × (present-day low solar activity)	100 × (present-day moderate solar activity)

Table 3. Solar flux parameters after Terada

A 3-D computational code is under development for the simulation of the exosphere motion and erosion into an inertial reference frame, bound to the planet surface. To image the interaction of the solar flux with the upper atmosphere of Mars, this interaction as given by the Terada simulations is presented in figure 5.

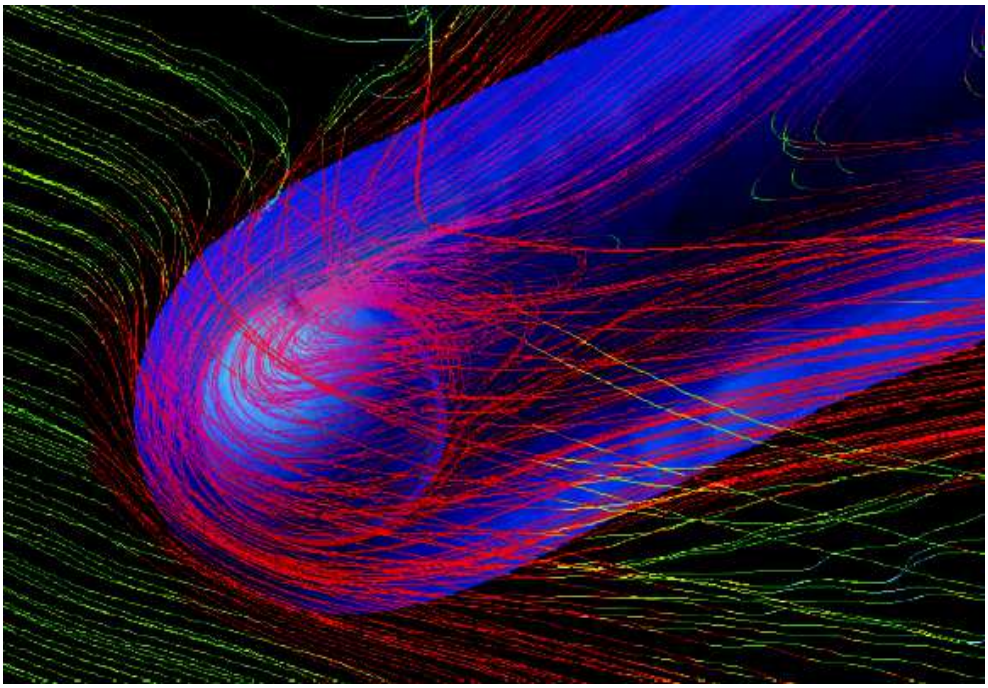

Fig. 5. Ion of O+ erosion simulated by Terada for a Mars atmosphere cca. 4.5 Ga ago. A density of $N(O^+)=100$ cm^{-3} is indicated with a blue transparent isosurface contour.

The authors of the simulation show that if they use the same assumption as Pérez-de-Tejada (1992) or Lammer *et al*. (2003b) that the cold ions are lost through the entire circular ring area around the planet's terminator, a maximum O+ loss rate of about 1.2×10^{29} s^{-1} is obtained. Integrating this loss rate over a period of Δt=150 million years, a maximum water loss equivalent to a global Martian ocean with a depth of 70 m is obtained, which is quite impressive and shows that the erosion of the atmosphere is extremely severe.

4. Solar-gravitational draught on Mars

The innovative model of the solar-gravitational air accelerator for use on Mars and other celestial bodies with thin atmosphere or without atmosphere is the closed circuit tower in figure 6.

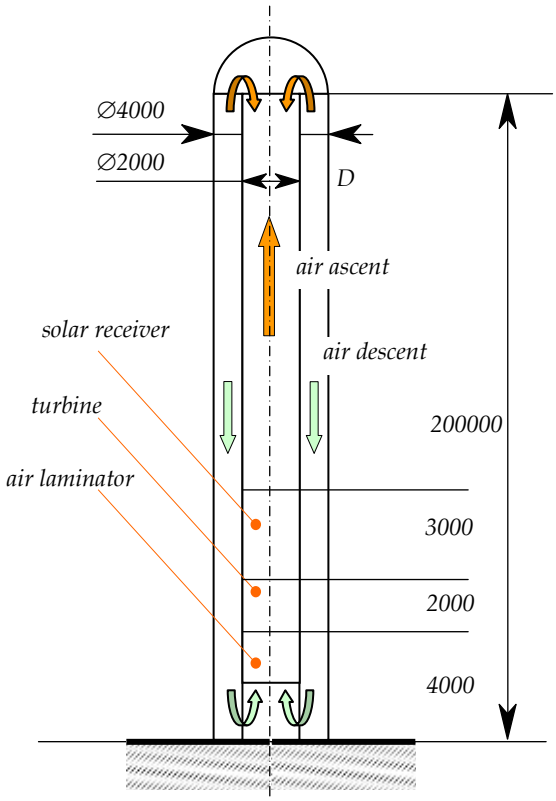

Fig. 6. Closed-circuit thermal-gravity tower for celestial bodies without atmosphere.

The air ascent tunnel is used as a heater with solar radiation collected through the mirror array, while the descent tunnels are used as air coolers to close the gravity draught.
According to the design in Fig. 6, a turbine is introduced in the facility next to the solar receiver, with the role to extract at least a part of the energy recovered from the solar radiation and to transmit it to the electric generator, for converting to electricity. The heat from the flowing air is thus transformed into mechanical energy with the payoff of a supplementary air rarefaction and cooling in the turbine.
The best energy extraction will take place when the air recovers entirely the ambient temperature before the solar heating, although this desire remains for the moment rather hypothetical. To search for the possible amount of energy extraction, the quotient ω is introduced, as further defined. Some differences appear in the theoretical model of the turbine system as compared to the simple gravity draught wind tunnel previously described.
The process of air acceleration at tower inlet is governed by the same energy (Bernoulli) incompressible (constant density ρ_0 through the process) equation as in the previous case,

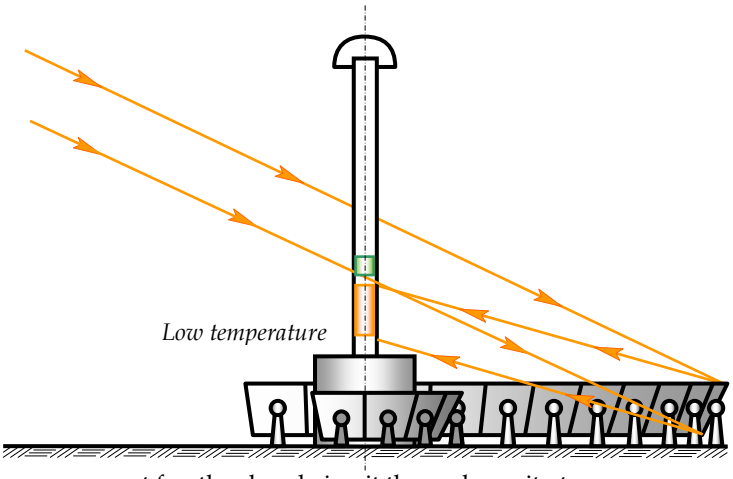

Fig. 7. Solar array concept for the closed-circuit thermal-gravity tower.

$$p_1 = p_0 - \frac{\dot{m}^2}{2\rho_0 A^2}\,. \tag{23}$$

The air is heated in the solar receiver with the amount of heat q, into a process with dilatation and acceleration of the airflow, accompanied by the usual pressure loss, called sometimes "*dilatation drag*" [8]. Considering a constant area cross-section in the heating solar receiver zone of the tube and adopting the variable γ for the amount of heating rather then the heat quantity itself,

$$\gamma = \frac{\rho_0 - \rho_2}{\rho_0} = 1 - \beta\,, \tag{24}$$

with a given value for

$$\beta = \frac{T_1}{T_2} < 1\,, \tag{25}$$

the continuity condition shows that the variation of the speed is given by

$$c_2 = c_1 / \beta\,. \tag{26}$$

No global impulse conservation appears in the tower in this case, as long as the turbine is a source of impulse extraction from the airflow. Consequently the impulse equation will be written for the heating zone only, where the loss of pressure due to the air dilatation occurs, in the form of eq. 27,

$$p_2 + \frac{\dot{m}^2}{\rho_2 A^2} = p_1 + \frac{\dot{m}^2}{\rho_0 A^2} - \Delta p_R\,. \tag{27}$$

A possible pressure loss due to friction into the lamellar solar receiver is considered through Δp_R. The dilatation drag is thus perfectly identified and the total pressure loss Δp_Σ from outside up to the exit from the solar heater is present in the expression

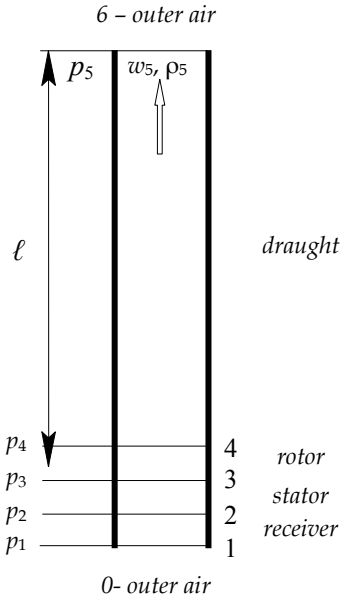

Fig. 8. Main stations in the turbine cold-air draught tower.

$$p_2 = p_0 - \frac{\dot{m}^2}{2\rho_0 A^2} - \frac{\dot{m}^2}{\rho_2 A^2} + \frac{\dot{m}^2}{\rho_0 A^2} - \Delta p_R \equiv p_0 - \Delta p_\Sigma \,. \tag{28}$$

Observing the definition of the rarefaction factor in (24) and using some arrangements the equation (28) gets the simpler form

$$p_2 = p_0 - \frac{\dot{m}^2}{\rho_0 A^2} \cdot \frac{\gamma + 1}{2(1-\gamma)} - \Delta p_R \,. \tag{29}$$

The thermal transform further into the turbine stator grid is considered as isentropic, where the amount of enthalpy of the warm air is given by

$$q = \frac{p_1}{\rho_1} \cdot \frac{1-\beta}{\beta} + \frac{\dot{m}^2}{\rho_1^2 A^2} \cdot \left[\frac{1 - \frac{\Gamma}{2}\beta}{\beta} + \frac{\frac{\Gamma}{2} - 1}{\beta^2} \right] - \frac{\Delta p_R}{\rho_1} \cdot \frac{1}{\beta} \,.$$

If the simplifying assumption is accepted that, under this aspect only, the heating progresses at constant pressure, then a far much simpler expression for the enthalpy fall in the stator appears,

$$\Delta h_{23} = \omega q = \omega c_p T_2 \gamma \,. \tag{30}$$

To better describe this process a choice between a new rarefaction ratio of densities ρ_3/ρ_2 or the energy quota ω must be engaged and the choice is here made for the later. Into the isentropic stator the known variation of thermal parameters occurs,

$$\frac{T_3}{T_2} = 1 - \omega\gamma \,, \tag{31}$$

$$\frac{p_3}{p_2} = (1 - \omega\gamma)^{\frac{\kappa}{\kappa-1}} \,, \tag{32}$$

$$\frac{\rho_3}{\rho_2} = (1 - \omega\gamma)^{\frac{1}{\kappa-1}} \,. \tag{33}$$

The air pressure at stator exit follows from combining (32) and (29) to render

$$p_3 = \left[p_0 - \frac{\dot{m}^2}{\rho_0 A^2} \cdot \frac{\gamma + 1}{2(1-\gamma)} - \Delta p_R \right] (1 - \omega\gamma)^{\frac{\kappa}{\kappa-1}} \,. \tag{34}$$

Considering a Zölly-type turbine the rotor wheel is thermally neutral and no variation in pressure, temperature and density appears. The only variation is in the air kinetic energy, when the absolute velocity of the airflow decreases from c_3 to $c_3 \sin\alpha_1$ and this kinetic energy variation is converted to mechanical work outside. Consequently $\rho_4 = \rho_3$, $p_4 = p_3$, $T_4 = T_3$ and

$$c_4 = \frac{c_1}{(1-\gamma)(1-\omega\gamma)^{\frac{1}{\kappa-1}}} \,. \tag{35}$$

The air ascent in the tube is only accompanied by the gravity up-draught effect due to its reduced density, although the temperature could drop to the ambient value. We call this quite strange phenomenon the *cold-air draught*. It is governed by the simple gravity form of Bernoulli's equation of energy,

$$p_5 = p_3 - g\rho_3 \ell \,. \tag{36}$$

The simplification was assumed again that the air density varies insignificantly during the tower ascent. The value for p_3 is here the one in (35). At air exit above the tower a sensible braking of the air occurs in compressible conditions, although the air density suffers insignificant variations during this process.
The Bernoulli equation is used to retrieve the stagnation pressure of the escaping air above the tower, under incompressible conditions

$$p_6{}^* = p_5 - \frac{\Gamma}{2}\rho_5 c_5^2 = p_5 + \frac{\Gamma}{2} \cdot \frac{\dot{m}^2}{\rho_3 A^2} = p_5 + \frac{\Gamma}{2} \cdot \frac{\dot{m}^2}{\rho_0 A^2} \cdot \frac{\rho_0}{\rho_3} \,. \tag{37}$$

Value for p_5 from (36) and for the density ratio from (24) and (33) are now used to write the full expression of the stagnation pressure as

$$\begin{aligned} p_6{}^* = (p_0 - \Delta p_R)(1 - \omega\gamma)^{\frac{\kappa}{\kappa-1}} - \frac{\dot{m}^2}{\rho_0 A^2} \cdot \frac{\gamma + 1}{2(1-\gamma)} \cdot (1 - \omega\gamma)^{\frac{\kappa}{\kappa-1}} + \\ + \frac{\dot{m}^2}{\rho_0 A^2} \cdot \frac{\Gamma}{2} \cdot \frac{1}{(1-\gamma) \cdot (1 - \omega\gamma)^{\frac{1}{\kappa-1}}} - g\rho_4 \ell \end{aligned} \tag{38}$$

It is observed again that up to this point the entire motion into the tower hangs on the value of the mass flow-rate, yet unknown. The mass flow-rate itself will manifest the value that fulfils now the condition of outside pressure equilibrium, or

$$p_6^* = p_0 - g\rho_0\ell \,. \tag{39}$$

This way the local altitude air pressure of the outside atmosphere equals the stagnation pressure of the escaping airflow from the inner tower. Introducing (38) in (39), after some re-arrangements the dependence of the global mass flow-rate along the tower, when a turbine is inserted after the heater, is given by the final developed formula:

$$R^2(\gamma) \equiv \frac{\dot{m}^2}{2g\ell\rho_0^2 A^2} = \frac{1-\gamma}{(\gamma+1)(1-\omega\gamma)^{\frac{\kappa+1}{\kappa-1}} - \Gamma}(1-\omega\gamma)^{\frac{1}{\kappa-1}}\left\{1-(1-\gamma)(1-\omega\gamma)^{\frac{1}{\kappa-1}} + \right. \\ \left. + \frac{p_0}{g\rho_0\ell}\left[(1-\omega\gamma)^{\frac{\kappa}{\kappa-1}} - 1\right] - \frac{\Delta p_R}{g\rho_0\ell}(1-\omega\gamma)^{\frac{\kappa}{\kappa-1}}\right\} \tag{40}$$

where the notations are again recollected

$\gamma = \dfrac{\rho_0 - \rho_2}{\rho_0}$, the dilatation by heating in the heat exchanger, previously denoted by *r*;

ω = the part of the received solar energy which could be extracted in the turbine;

Δp_R = pressure loss into the heater and along the entire tube either.

All other variables are already specified in the previous chapters. It is clearly noticed that by zeroing the turbine effect (ω = 0) the formula (40) reduces to the previous form, or by neglecting the friction, which stays as a validity check for the above computations. For different and given values of the efficiency ω the variation of the mass flow-rate through the tube depends parabolically of the rarefaction factor γ.

Notice must be made that the result in (40) is based on the convention (30). The exact expression of the energy *q* introduced by solar heating yet does not change this result significantly. Regarding the squared mass flow-rate itself in (40), it is obvious that the right hand term of its expression must be positive to allow for real values of R^2. This only happens when the governing terms present the same sign, namely

$$\left\{(\gamma+1)(1-\omega\gamma)^{\frac{\kappa+1}{\kappa-1}} - \Gamma\right\}\cdot\left\{1-(1-\gamma)(1-\omega\gamma)^{\frac{1}{\kappa-1}} + \frac{p_0}{g\rho_0\ell}\left[(1-\omega\gamma)^{\frac{\kappa}{\kappa-1}} - 1\right] - \frac{\Delta p_R}{g\rho_0\ell}(1-\omega\gamma)^{\frac{\kappa}{\kappa-1}}\right\} : 0 \,. \tag{41}$$

The larger term here is the ratio $p_0/(g\rho_0\ell)$, which always assumes a negative sign, while not vanishing. The conclusion results that the tower should surpass a minimal height for a real R^2 and this minimal height were quite huge. Very reduced values of the efficiency ω should be permitted for acceptably tall solar towers. This behavior is nevertheless altered by the first factor in (41) which is the denominator of (30) and which may vanish in the usual range of rarefaction values γ. A sort of thermal resonance appears at those points and the turbine tower works properly well.

5. Reasons and costs for terraforming Mars

Thicken Mars' atmosphere, and make it more like Earth's. Earth's atmosphere is about 78% Nitrogen and 21% Oxygen, and is about 140 times thicker than Mars' atmosphere. Since Mars

is so much smaller than Earth (about 53% of the Earth's radius), all we'd have to do is bring about 20% of the Earth's atmosphere over to Mars. If we did that, not only would Earth be relatively unaffected, but the Martian atmosphere, although it would be thin (since the force of gravity on Mars is only about 40% of what it is on Earth), would be breathable, and about the equivalent consistency of breathing the air in Santa Fe, NM. So that's nice; breathing is good.

Mars needs to be heated up, by a lot, to support Earth-like life. Mars is cold. Mars is damned cold. At night, in the winter, temperatures on Mars get down to about -160 degrees! (If you ask, "Celcius or Fahrenheit?", the answer is first one, then the other.) But there's an easy fix for this: add greenhouse gases. This has the effect of letting sunlight in, but preventing the heat from escaping. In order to keep Mars at about the same temperature as Earth, all we'd have to do is add enough Carbon Dioxide, Methane, and Water Vapor to Mars' atmosphere. Want to know something neat? If we're going to move 20% of our atmosphere over there, we may want to move 50% of our greenhouse gases with it, solving some of our environmental problems in the process.

These greenhouse gases would keep temperatures stable on Mars and would warm the planet enough to melt the icecaps, covering Mars with oceans. All we'd have to do then is bring some lifeforms over and, very quickly, they'd multiply and cover the Martian planet in life. As we see on Earth, if you give life a suitable environment and the seeds for growth/regrowth, it fills it up very quickly.

So the prospects for life on a planet with an Earth-like atmosphere, temperature ranges, and oceans are excellent. With oceans and an atmosphere, Mars wouldn't be a red planet any longer. It would turn blue like Earth! This would also be good for when the Sun heated up in several hundred million years, since Mars will still be habitable when the oceans on Earth boil. But there's one problem Mars has that Earth doesn't, that could cause Mars to lose its atmosphere very quickly and go back to being the desert wasteland that it is right now: Mars doesn't have a magnetic field to protect it from the Solar Wind. The Earth's magnetic field, sustained in our molten core, protects us from the Solar Wind.

Mars needs to be given a magnetic field to shield it from the Solar Wind. This can be accomplished by either permanently magnetizing Mars, the same way you'd magnetize a block of iron to make a magnet, or by re-heating the core of Mars sufficiently to make the center of the planet molten. In either case, this allows Mars to have its own magnetic field, shielding it from the Solar Wind (the same way Earth gets shielded by our magnetic field) and allowing it to keep its atmosphere, oceans, and any life we've placed there.

But this doesn't tell us how to accomplish these three things. The third one seems to us to be especially difficult, since it would take a tremendous amount of energy to do. Still, if you wanted to terraform Mars, simply these three steps would give you a habitable planet.

The hypothetical process of making another planet more Earth-like has been called terraforming, and terraforming Mars is a frequently mentioned possibility in terraforming discussions. To make Mars habitable to humans and earthly life, three major modifications are necessary. First, the pressure of the atmosphere must be increased, as the pressure on the surface of Mars is only about 1/100th that of the Earth. The atmosphere would also need the addition of oxygen. Second, the atmosphere must be kept warm. A warm atmosphere would melt the large quantities of water ice on Mars, solving the third problem, the absence of water.

Terraforming Mars by building up its atmosphere could be initiated by raising the temperature, which would cause the planet's vast CO_2 ice reserves to sublime and become atmospheric gas. The current average temperature on Mars is −46 °C (-51 °F), with lows of −87 °C (-125 °F), meaning that all water (and much carbon dioxide) is permanently frozen. The easiest way to raise the temperature seems to be by introducing large quantities of CFCs

(chlorofluorocarbons, a highly effective greenhouse gas) into the atmosphere, which could be done by sending rockets filled with compressed CFCs on a collision course with Mars. After impact, the CFCs would drift throughout Mars' atmosphere, causing a greenhouse effect, which would raise the temperature, leading CO_2 to sublimate and further continuing the warming and atmospheric buildup. The sublimation of gas would generate massive winds, which would kick up large quantities of dust particles, which would further heat the planet through direct absorption of the Sun's rays. After a few years, the largest dust storms would subside, and the planet could become habitable to certain types of algae and bacteria, which would serve as the forerunners of all other life. In an environment without competitors and abundant in CO_2, they would thrive. This would be the biggest step in terraforming Mars.

6. Conclusion

The problem of creating a sound source of energy on Mars is of main importance and related to the capacity of transportation from Earth to Mars, very limited in the early stages of Mars colonization, and to the capacity of producing the rough materials in situ. Consequently the most important parameter that will govern the choice for one or another means of producing energy will be the specific weight of the powerplant. Besides the nuclear sources, that most probably will face major opposition for a large scale use, the only applicable source that remains valid is the solar one. As far as the solar flux is almost four times fainter on Mars than on Earth, the efficiency of PVC remains very doubtfull, although it stands as a primary candidate. This is why the construction of the gravity assisted air accelerators looks like a potential solution, especially when rough materials will be available on Mars surface itself. The thermal efficiency of the accelerator for producing a high power draught and the propulsion of a cold air turbine remains very high and attractive. The large area of the solar reflector array is still one of the basic drawbacks of the system, that only could be managed by creating very lightweight solar mirrors, but still very stiff to withstand the winds on Mars surface.

7. References

*** (1977), Scientific Results of the Viking Project, *Journal of Geophysical Research*, vol. 82, no. 28, A.G.U., Washington, D.C.

*** *The Astronomical Almanac*, 2010, U.S. Naval Observatory and H.M. Nautical Almanac Office.

Michael Allison and Megan McEwen, 2000. A post-Pathfinder evaluation of aerocentric solar coordinates with improved timing recipes for Mars seasonal/diurnal climate studies. Planetary and Space Science, 48, 215-235.

Asimov, Isaac (1979), *Civilisations extraterrestres*, Ed. L'Etincelle, Montreal, Quebec, Canada.

Andre L. Berger, 1978. Long Term Variations of Daily Insolation and Quaternary Climatic Changes. Journal of the Atmospheric Sciences, volume 35(12), 2362-2367.

Berger A and Loutre MF, 1992. Astronomical solutions for paleoclimate studies over the last 3 million years. Earth and Planetary Science Letters, 111, 369-382.

Bibring, J.P., and 42 others (2006), Global mineralogical and aqueous Mars history derived from OMEGA/Mars Express data, *Science*, vol. 312, pp. 400–404.

P. Bizony (1998), *The Exploration of Mars-Searching for the Cosmic Origins of Life*, Aurum Press, London.

David Brain (2008), ESA observations indicate Mars and Venus are surprisingly similar, *Thaindian News*, March 6th <esa-observations-indicate-mars-and-venus-are-surprisingly-similar_10024474.html>.

Bullock, M. A., and J. M. Moore (2007), Atmospheric conditions on early Mars and the missing layered carbonates, *Geophys. Res. Lett.*, 34, L19201, doi:10.1029/2007GL030688.

Sylvio Ferraz-Mello (1992), Chaos, resonance, and collective dynamical phenomena in the solar system, *Proceedings of the 152nd Symposium of the IAU*, Angra dos Reis, Brazil, July 15-19, 1991, Springer, ISBN 0792317823, 9780792317821, 416 pp.

Flammarion, Nicolas Camille (1862), *La pluralité des mondes habités*, Didier, Paris.

Jones, Barrie W. (2008), Mars before the space age, *International Journal of Astrobiology*, Volume 7, Number 2, 143-155.

McGovern, Patrick J., and Morgan, Julia K. (2009), Mars Volcanic spreading and lateral variations in the structure of Olympus Mons, *Geology*, 37, pp 139-142.

D. Mortari, "*On the Rigid Rotation Concept in n-Dimensional Spaces*" Journal of the Astronautical Sciences, vol. 49, no. 3, July-September 2001.

Oparin, A. I. and Fesenkov, V. G. (1956), *Jizni vo vselennoi* (*Life in Universe*-Russ.), Ed. Academy of Science of USSR.

Phillips, R.J., Zuber, M.T., Solomon, S.C., Golombek , M.P., Jakosky, B.M., Banerdt, W.B., Smith, D.E., Williams, R.M.E., Hynek, B.M., Aharonson , O., and Hauck, S.A. (2001), Ancient geodynamics and global-scale hydrology on Mars: *Science*, vol. 291, pp. 2587–2591.

Rugescu, R. D. (2003), Sound Pressure Behavior in Relative Fluid Mechanics, *Proceedings of the 10th International Congress on Sound and Vibration (ICSV10)*, Stockholm, Sweden, July 7-10, pp. 3169-3176.

Rugescu, R. D. (2000), *On the Principles of Relative Motion of Continua*, Scientific Bulletin of U.P.B., series A (Applied Mathematics and Physics), 62, 2/2000, pp. 97-108;

Schubert, G., Russell, C.T., and Moore, W.B. (2000), Timing of the martian dynamo, *Nature* 408, pp. 666–667.

Sheehan, W. (1996), *The Planet Mars: A History of Observation & Discovery*, University of Arizona Press.

Smith, D. E., Lerch, F. J., Nerem, R. S., Zuber, M. T., Patel, G. B., Fricke, S. K., Lemoine, F. G. (1993), An Improved Gravity Model for Mars: Goddard Mars Model 1, Journal of Geophysical Research (ISSN 0148-0227), vol. 98, no. E11, p. 20, 871-889.

Standish, E. M. (1998), JPL IOM 312.F-98-048, (DE405/LE405 Ephemeris).

Terada, N., Kulikov, Y. N., Lammer, H., Lichtenegger, H. I. M., Tanaka, T., Shinagawa, H., & Zhang, T. (2009), Atmosphere and Water Loss from Early Mars Under Extreme Solar Wind and Extreme Ultraviolet Conditions, *Astrobiology*, Vol. 9, No. 1, 2009, © Mary Ann Liebert, Inc., DOI: 10.1089/ast.2008.0250

C. Tulita, S. Raghunathan, E. Benard, *Control of Steady Transonic Periodic Flow on NACA-0012 Aerofoil by Contour Bumps*, Department of Aeronautical Engineering, The Queen's University of Belfast, Belfast, Northern Ireland, United Kingdom, 2002;

Synge, J. L., and Griffith, B. A., (1949), Principles of Mechanics, second ed., McGraw-Hill Book Company, Inc., New York, Toronto, London.

Wood, B.E., Müller, H.-R., Zank, G.P., Linsky, J.L., and Redfield, S. (2005) New mass-loss measurements from astrospheric Ly-α absorption, *Astrophys. J.*, 628:L143–L146.

Zhang, M.H.G., Luhmann, J.G., Nagy, A.F., Spreiter, J.R., and Stahara, S.S. (1993), Oxygen ionization rates at Mars and Venus: relative contributions of impact ionization and charge exchange. *J. Geophys. Res.*, 98, pp. 3311–3318.

Solar Energy

Edited by Radu D Rugescu

ISBN 978-953-307-052-0
Hard cover, 432 pages
Publisher InTech
Published online 01, February, 2010
Published in print edition February, 2010

The present “Solar Energy” science book hopefully opens a series of other first-hand texts in new technologies with practical impact and subsequent interest. They might include the ecological combustion of fossil fuels, space technology in the benefit of local and remote communities, new trends in the development of secure Internet Communications on an interplanetary scale, new breakthroughs in the propulsion technology and others. The editors will be pleased to see that the present book is open to debate and they will wait for the readers’ reaction with great interest. Critics and proposals will be equally welcomed.

How to reference

In order to correctly reference this scholarly work, feel free to copy and paste the following:

Dragos Ronald Rugescu and Radu Dan Rugescu (2010). Potential of the Solar Energy on Mars, Solar Energy, Radu D Rugescu (Ed.), ISBN: 978-953-307-052-0, InTech, Available from: http://www.intechopen.com/books/solar-energy/potential-of-the-solar-energy-on-mars

INTECH
open science | open minds

InTech Europe
University Campus STeP Ri
Slavka Krautzeka 83/A
51000 Rijeka, Croatia
Phone: +385 (51) 770 447
Fax: +385 (51) 686 166
www.intechopen.com

InTech China
Unit 405, Office Block, Hotel Equatorial Shanghai
No.65, Yan An Road (West), Shanghai, 200040, China
中国上海市延安西路65号上海国际贵都大饭店办公楼405单元
Phone: +86-21-62489820
Fax: +86-21-62489821